J. Am. Soc. Mass Spectrom. (2018) 29:1012–1020
DOI: 10.1007/s13361-018-1899-9

RESEARCH ARTICLE

Single-Cell Mass Spectrometry Reveals Changes in Lipid and Metabolite Expression in RAW 264.7 Cells upon Lipopolysaccharide Stimulation

Bo Yang,[1,2] Nathan Heath Patterson,[1,2] Tina Tsui,[1,2] Richard M. Caprioli,[1,2,3] Jeremy L. Norris[1,2,3]

[1]Mass Spectrometry Research Center, Vanderbilt University, 465 21st Avenue South, Nashville, TN 37240, USA
[2]Department of Biochemistry, Vanderbilt University School of Medicine, 465 21st Avenue South, Nashville, TN 37240, USA
[3]Department of Chemistry, Vanderbilt University, 465 21st Avenue South, Nashville, TN 37240, USA

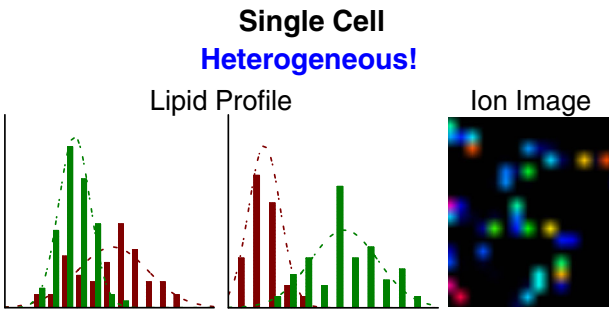

Abstract. It has been widely recognized that individual cells that exist within a large population of cells, even if they are genetically identical, can have divergent molecular makeups resulting from a variety of factors, including local environmental factors and stochastic processes within each cell. Presently, numerous approaches have been described that permit the resolution of these single-cell expression differences for RNA and protein; however, relatively few techniques exist for the study of lipids and metabolites in this manner. This study presents a methodology for the analysis of metabolite and lipid expression at the level of a single cell through the use of imaging mass spectrometry on a high-performance Fourier transform ion cyclotron resonance mass spectrometer. This report provides a detailed description of the overall experimental approach, including sample preparation as well as the data acquisition and analysis strategy for single cells. Applying this approach to the study of cultured RAW264.7 cells, we demonstrate that this method can be used to study the variation in molecular expression with cell populations and is sensitive to alterations in that expression that occurs upon lipopolysaccharide stimulation.

Keywords: MALDI, Imaging mass spectrometry, Single cell, Lipids and metabolites, Heterogeneity

Received: 16 November 2017/Revised: 14 January 2018/Accepted: 22 January 2018/Published Online: 13 March 2018

Introduction

Current understanding about the biochemistry of the cell is primarily based upon measurements of individual chemical components extracted from populations of cells either grown in culture or excised from tissue. The limited capabilities of analytical technologies previously available to researchers studying the chemistry of living systems have generally only allowed these measurements to be applied to large sample sizes derived from thousands-to-millions of cells such that a sufficient amount of the analytes of interest can be isolated. Recently, there is a growing appreciation that although cells may appear to function in a similar manner and morphologically may not exhibit any distinguishing features, individual cells can have varying expression patterns for their constituent biomolecules based upon their environment and the signals obtained from external stimuli [1–3]. This recognition, along with an increasingly sensitive suite of analytical tools, has provided the motivation to probe the molecular makeup of individual cells and collect single cell measurements for even large cell populations [4]. There have now been many demonstrations that individual cells often have biochemical compositions that can differ significantly from the population average based upon the influence of individual microenvironmental factors. This

Electronic supplementary material The online version of this article (https://doi.org/10.1007/s13361-018-1899-9) contains supplementary material, which is available to authorized users.

Correspondence to: Jeremy Norris; *e-mail:* j.norris@vanderbilt.edu

phenomenon is believed to be a fundamental part of survival and aid in the proliferation of bacterial colonies [5]. Furthermore, in multicellular organisms, cellular heterogeneity has also been reported in the development of functional tissues and organ systems, immune response [6, 7], and cancer progression [8, 9]. Therefore, tools and technologies that facilitate the characterization of biological processes that occur at the single cell level are ultimately required in order to develop full understanding of human health and disease.

There are several analytical technologies now being applied to the analysis of single cells. Sequencing technologies provide the sophistication (e.g., throughput and sensitivity) to begin to measure gene and transcription-level variation at the single cell level [10]. Though less developed, recent advances in mass spectrometry (MS) technologies and methods have opened up single-cell analyses to other analyte classes, including peptides and metabolites. The range of mass spectrometry methods developed to study single cells includes secondary ion mass spectrometry (SIMS) [11–14], laser ablation electrospray ionization MS (LAESI) [15], capillary electrophoresis-electrospray ionization (CE-ESI) MS [16–18], live single-cell (SC) MS [19, 20], single probe MS [21–23], and matrix-assisted laser desorption ionization (MALDI) MS [24, 25]. Each of the MS techniques has advantages with some significant limitations for single-cell analysis. For example, desorption-ionization techniques like SIMS and LAESI provide the high spatial resolution required to sample individual cells with minimal sample preparation, but each approach suffers from limited chemical specificity due to fragmentation during the ionization process.

There are also various approaches that have adapted chromatographic or electrophoretic techniques to extract and/or separate the contents of a single cell for mass spectrometric analysis. This approach has the advantage that the separation significantly increases the number of species that can be sampled from the cell. However, positioning of a single cell for sampling the contents into the analytical system requires tedious manual work or sophisticated micromanipulation systems [26]. Furthermore, the analysis time required for each individual cell is several minutes, reducing the number of cells that can be practically sampled in a single experiment and thus the statistical power of the analysis. In contrast, recent work employing targeted MALDI analysis of single cells on a plate performed using a histology-directed workflow can increase the number of cells that can be analyzed. This approach leverages the speed of laser-based ionization to sample a larger number of cells [4]. However, this study was limited in focus to a small set of known peptides.

In this study, we present a workflow for single-cell analysis (Figure 1) based on imaging mass spectrometry (IMS) using a Fourier transform ion cyclotron resonance mass spectrometer (FTICR MS) for the measurement of low molecular weight metabolites and lipids. In order to demonstrate the capabilities of this approach, the platform was used in the analysis of normal and lipopolysaccharide (LPS)-treated single RAW 264.7 macrophage cells. Upon exposure to LPS, a conserved component of the Gram-negative bacterium's outer membrane, RAW 264.7 macrophage cells release a large number of immunoregulatory molecules that recruit and activate other immune cells to help fight the infection [27, 28]. The speed of MALDI-IMS enables high spatial resolution and high throughput single-cell analysis. Combined with the high sensitivity of FTICR MS, hundreds of metabolites and lipids can be measured from a large population (> 100) of single cells in hours to investigate the influence of LPS stimulation on heterogeneity of molecular expressions. This workflow includes strategies for the preparation of cells for single cell MALDI analysis, recommendations for data acquisition, and software that permits the extraction of single-cell data from images and analysis of the heterogeneity for molecular expression for each molecule in the sample.

Experimental Setup

Cell Handling and Sample Preparation

The overall workflow summarized in Figure 1 includes cell handling and MALDI sample preparation steps. RAW 264.7 cells are obtained from ATCC (Manassas, VA) and cultured in Dulbecco's modified Eagle's medium (DMEM, Gibco) with 10% *v/v* heat-inactivated fetal bovine serum (Atlanta Biologicals) and 1% *v/v* penicillin/streptomycin (P/S) (Gibco) at 37 °C with 5% CO_2 atmosphere. Five sterile indium tin oxide (ITO)-coated glass slides (Delta Technologies) are placed in a tissue culture flask with removable lid (TPP). Cells are seeded at 6×10^5 cells/mL. For the LPS stimulation, normal cells are exposed to 100 ng/mL LPS for 16 h prior to plating. The cell slides are collected after 8 h and washed with PBS buffer twice to remove cell culture media. The cell slides are snap-frozen in liquid nitrogen and stored at − 80 °C until analysis.

On the day of analysis, the cell slides are stored under vacuum in a desiccator for 30 min to prevent moisture condensation during thawing of the cells and hence reduce delocalization of analytes on surface. The cells are then rinsed by sequentially dipping the slides into a Petri dish filled with 150 mM cold ammonium formate for 30 s to remove salts from the cells and increase signal intensities of lipids and metabolites. Excess ammonia formate on the slide is quickly removed by wiping with Kimwipes. After rinsing, the cell slides are stored in a desiccator for 30–60 min to allow solvent to dry. Fiducial points are placed on the slides before image scanning. Scanning is performed before application of matrix to obtain a clear image of the cells. Slide images are obtained at × 5 magnification using a Leica Image Scanner and converted to the JPEG format. Application of the MALDI matrix is performed using a custom-built sublimation apparatus as previously described [29]. The core condenser sleeve was purchased from Chemglass Life Sciences and fits a plate diameter of 70 mm. About 100 mg of 1,5-diaminonaphthalene (DAN) MALDI matrix was placed at the bottom of the condenser sleeve. The pressure inside the condenser sleeve was held at

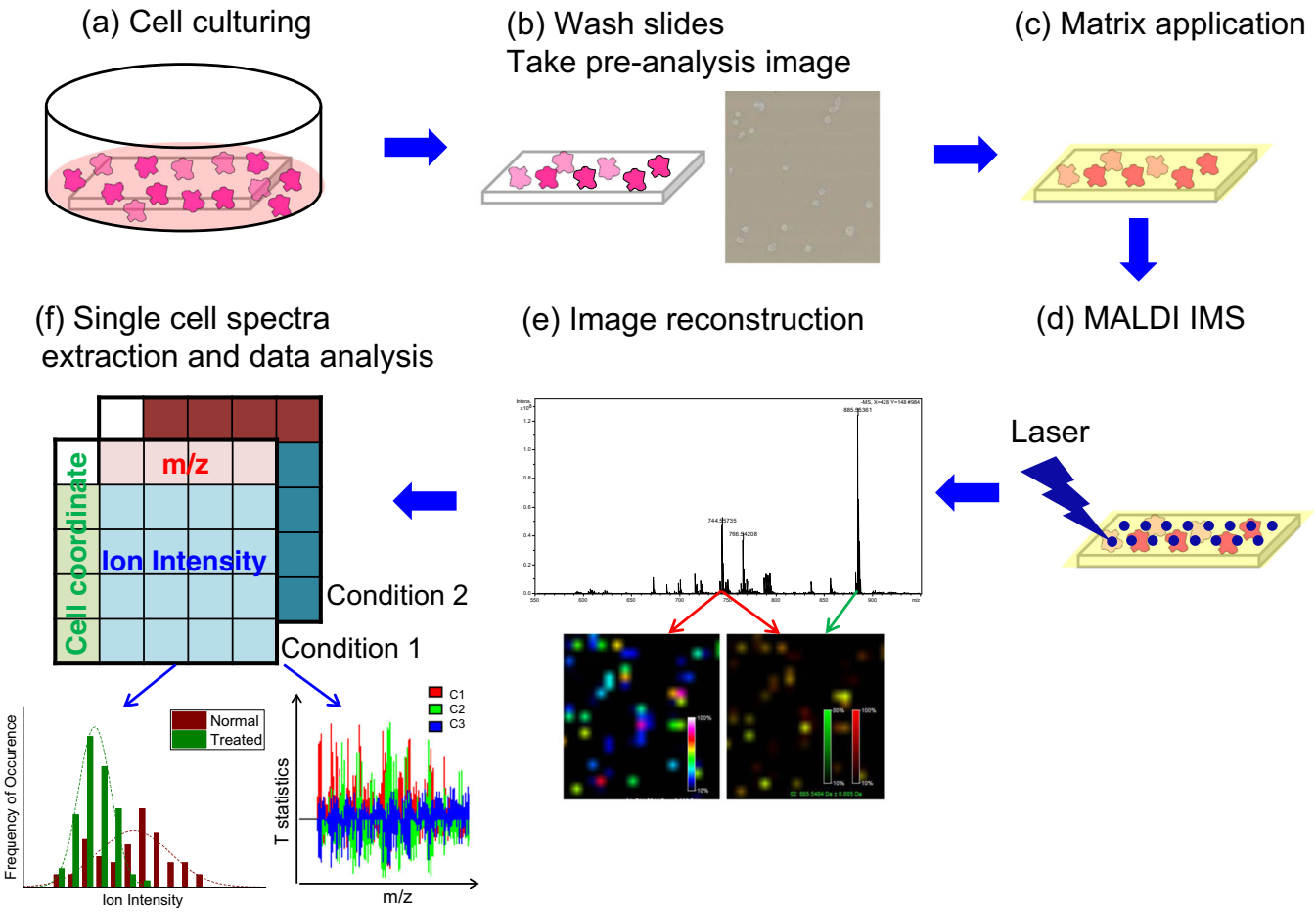

Figure 1. Single-cell analysis performed by imaging mass spectrometry. (a) Raw 264.7 cells are grown on glass microscope slides; multiple growth conditions can be used to examine their influence on single cell molecular expression. (b) The glass slide is removed from media, and the adherent cells are washed to remove residual culture media. Cells are imaged in a slide scanner to record their relative position on the plate. (c) MALDI matrix is applied to the sample target. (d) MALDI-IMS is performed by rastering the laser across the field of cells, recording mass spectra at each discrete location. (e) Ion abundance data can be extracted to visualize differences in cellular expression across the cell population. MALDI ion images are registered to the optical image. (f) Mass spectra that were acquired from single cells are extracted. The individual ion abundances are extracted to facilitate further analysis and visualization

< 40 mTorr by a rough pump and monitored by a digital thermocouple vacuum gauge controller. The condenser sleeve was placed on a sand bath heated by a hot plate. Sublimation for the single cell application was optimized by varying temperature and time parameters. Six minutes at a temperature of ~ 105 °C was found to be optimal.

After sublimation, matrix recrystallization is performed using a normal Petri dish to enhance signal intensities of lipids and metabolites [30]. The slide with sublimated matrix is attached to a copper plate, which is taped to the underside of the lid of the Petri dish. A matrix recrystallization solution is pipetted onto a piece of filter paper placed in the bottom part of the Petri dish. The Petri dish is reassembled and sealed using PetriSeal tape to create a hydration chamber. The Petri dish is placed in an oven preheated to 85 °C for 2 min, and then opened to allow the slide to dry in the oven.

MALDI Imaging and CASI Experiments

Imaging experiments were performed using a Bruker solariX 15T MALDI/ESI-FTICR (Bruker Daltonics, Bremen, Germany) equipped with a 355 nm Smartbeam II laser operated at 1000 Hz. The mass spectrometer was first calibrated for high mass accuracy using Agilent ESI tuning mix. Laser beam size is measured as 20–25 µm. Laser raster size is defined as 25 µm. Images were acquired with an average of 500 laser shots/pixel in negative ion mode and in the mass range of *m/z* 500–1500. Images were generated using FlexImaging 4.0 (Bruker Daltonics, Billerica, MA, USA). Continuous accumulation of selected ion (CASI) experiments were performed on replicate slides. CASI isolation mass is optimized and set to *m/z* 650 with a window width of 250. Each imaging acquisition requires approximately 1 h of instrument time using the current settings.

MALDI Data Extraction and Processing

After MALDI-IMS data acquisition, the raw IMS file is converted to MATLAB format using a custom-developed Web-based interface so that it can be analyzed using common data processing tools or transferred to biostatisticians for analysis. An automated custom graphical user interface (Figure 2) was developed to extract single-cell mass spectra from the whole MALDI-IMS dataset. The high-resolution bright-field cell image acquired prior to IMS analysis is loaded into the software, shown in Figure 2b. The positions of the cells are automatically identified, and the corresponding pixels are marked by the green circles. Coordinates of each pixel are calculated using the coordinates of the four corners of the analyzed region indicated by the white dashed-line box in the image. Coordinates of all pixels corresponding to cell positions are listed in Figure 2d. Each pixel can be selected or unselected by clicking the box next to its coordinates in Figure 2d or by directly clicking the green circles in Figure 2b. Single mass spectra corresponding to selected pixels are shown in Figure 2a. In some cases, one cell spreads across several pixels. Selected single spectra are extracted as Bruker .xy files using the export function. Extracted single-cell mass spectra are normalized to total ion current (TIC), and then peak picked based on a 12% intensity threshold. To assist identifications of lipids and metabolites, peak picked mass list is searched against Lipid Maps Structure Database (LMSD) and METLIN metabolite database using a mass tolerance of 15 ppm.

PCA Analysis of Single-Cell Mass Spectra

The IMS data previously converted to a MATLAB format was accessed in R. The previously selected single-cell spectra were then extracted by their *x*,*y* coordinate indices and loaded into the *Cardinal* R package's IMS container with in-house scripts [31]. From here, PCA was performed using Cardinal with 100 components, centering, and the IRLBA algorithm for singular value decomposition calculation. Visualization of the single cells' PCA score plots as 2D scatter plots was used to determine which PCs best separated the treated versus normal single cells. The loading plots of the PCs demonstrating the best separation of these groups were further queried for differentially expressed signals.

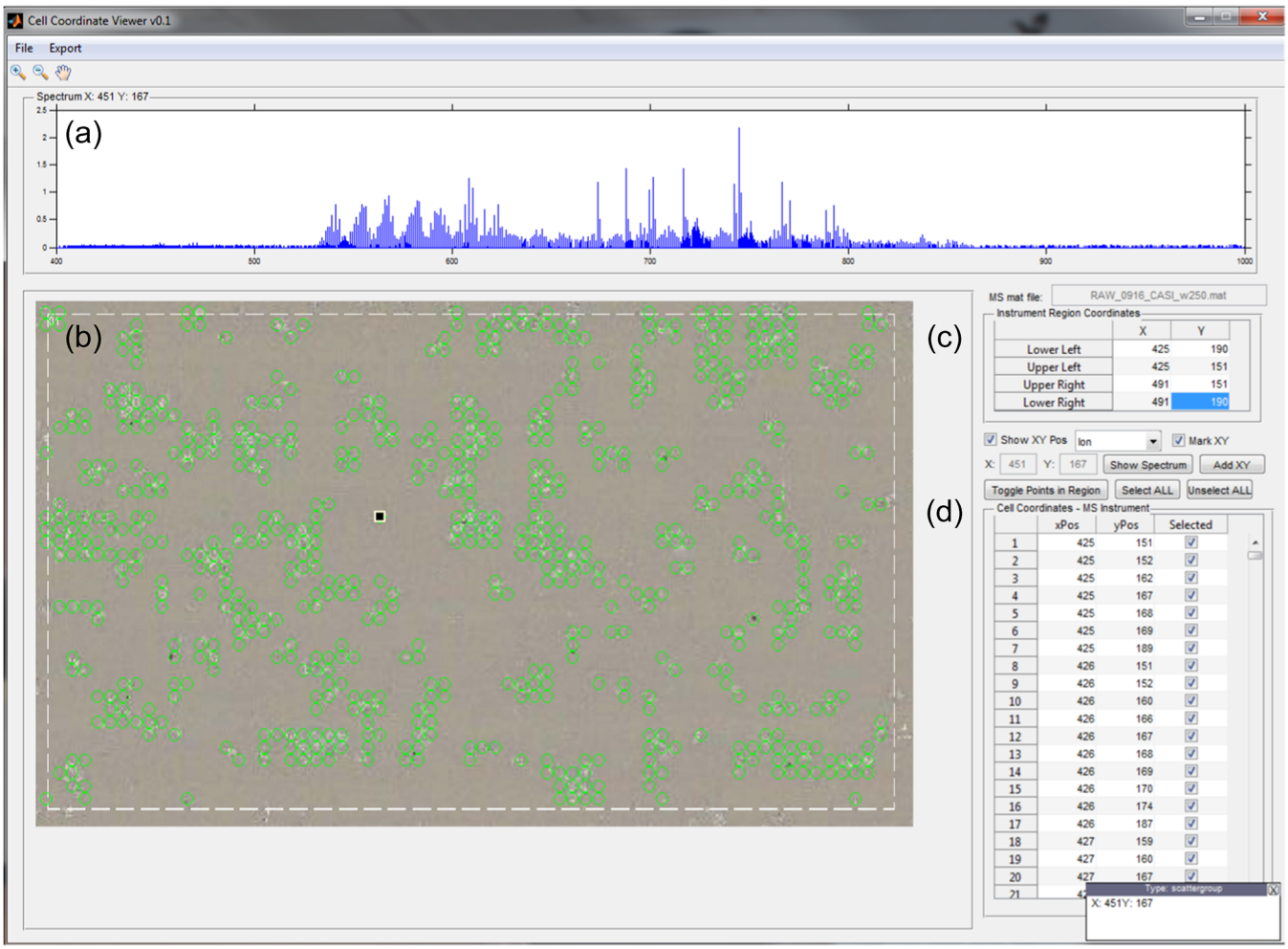

Figure 2. Screen capture of the single cell spectra extraction software. (A) Spectrum display of a selected position. (B) Pre-analysis cell image. Green circles are single pixels corresponding to identified cell positions. (C) Coordinates of the four corners of analyzed region indicated by the white dashed-line box. (D) Coordinates of pixels

Results and Discussions

Single Cell Mass Spectrometry Analysis of Normal RAW 264.7 Cells

Figure 3a displays a bright-field cell image acquired prior to IMS analysis, and Figure 3b shows a representative ion image corresponding to *m/z* 885.55 acquired from the same region. In this study, the spatial resolution of the IMS experiment was set to 25 μm. The goal of these experiments was to collect a large number of lipid/metabolite expression profiles from the cell population. RAW 264.7 cells are approximately 10–15 μm in diameter; however, in this experiment, the distance between the cells in culture was often greater than 100 μm. Thus, by using a beam diameter larger than the cell size, we were able to increase the number of cells in the analysis. Cells that were only partially ablated by the laser and spectra that were collected from multiple cells were eliminated using visual inspection and not considered in the final analysis.

The variation in ion abundance across the whole cell population, observed in the ion image shown in Figure 3b, indicates that expression of this lipid is spatially heterogeneous. Guided by the bright-field cell image, positions of single cells are identified and the corresponding single pixel spectra are extracted from the ion image as single-cell mass spectra. In this experiment, 60 mass spectra are extracted from individual single cells in the normal data set acquired as part of a 1-h IMS run. The number of mass spectra extracted can easily be increased by acquiring images from a larger area, given the MALDI matrix remains stable. Representative spectra extracted from two individual single cells sampled in this analysis are also shown in Figure 3. Using the Bruker solariX 15T MALDI-FTICR-MS, we detected 670 distinct signals in the mass range between *m/z* 525–775 Da. Within this group of 670 ions, 334 of them match with known compounds in the LMSD or METLIN databases with a mass tolerance of 15 ppm. The relative intensities of the peaks corresponding to *m/z* = 744.55 and 885.55 in Figure 3c and d vary dramatically from one cell to the other, illustrating heterogeneity of lipid and metabolite expressions within this cell population.

Comparison of Normal and LPS-Stimulated Cells

In order to investigate if this analytical approach can detect changes in the molecular heterogeneity of lipid and metabolite expression induced by chemical stimulation of cells, we performed parallel experiments on LPS-stimulated RAW 264.7 cells. To minimize any differences in detection or expression of lipids and metabolites caused by sample preparation and instrument performance, the LPS-stimulated RAW 264.7 cell slides were prepared in parallel with the normal cell slide on the same day using the same reagent. Both slides were analyzed sequentially on the same day using same instrument method. The MALDI-IMS data obtained from the LPS-stimulated cells are processed using same procedures described previously to extract single-cell spectra. We performed principle component analysis (PCA) on the single-cell data to identify latent molecular signatures in the data. The PCA analysis of the single-cell groups revealed multivariate differences between the two cell conditions in the third principal component (Figure 4a) which described ~ 7% of the dataset's variance. Examining this principal component's loadings, many features were found to be differential between the two groups (Figure 4b). Lipid species with high loading scores are putatively identified using accurate mass and listed in Table 1. Even though the exact structures of these lipids has not been determined, it is still worth noting that the levels of phospholipids with a low degree of unsaturation (e.g., PI(36:1), PI(36:2), PE(36:1), PE(36:2), and PA(36:2)) are significantly increased upon LPS stimulation, whereas the levels of lipids with a high degree of unsaturation (e.g., PI(40:5), PI(38:4), PE(38:4), and PE(36:4)) are significantly decreased upon LPS stimulation. Similar trends were observed by Guo et al. in the cancer microenvironment compared with the adjacent normal tissue for six different types of cancer (e.g., breast, lung, colorectal, esophageal, gastric, and thyroid cancer) [32]. Sphingolipids such as SM(d18:0/15:0) is more prevalent in normal compared to LPS-treated RAW 264.7 cells. This trend has also been observed between normal and glaucomatous aqueous humor [33]. However, the specific role of these lipids in cellular or biological function is largely unclear. To understand how LPS stimulation influences the heterogeneities of lipid and metabolite expressions from single cells, histograms of ion abundances corresponding to *m/z* = 885.55 (PI(36:4)), 861.55 (PI(36:2)), and 777.56 (PG(36:0)) were plotted for normal and LPS-stimulated RAW 264.7 cells (Figure 5). These histograms illustrate the intensity distributions of each ion across the cell population investigated. As can be seen from Figure 5a, the signal of ion at *m/z* = 885.55 (PI(36:4)) is downregulated and the distribution became narrower, indicating that expression of this species is less heterogeneous upon LPS stimulation. In contrast, the signal of ion corresponding to *m/z* = 861.55 (PI(36:2)) is upregulated and the distribution became broader upon LPS stimulation (Figure 5b), whereas the signal and intensity distribution of ion corresponding to *m/z* = 777.56 (PG(36:0)) is largely unchanged (Figure 5c). The up- or downregulation of specific lipids or metabolites can, in most cases, be easily measured from population-level cell analysis experiments. However, the changes in overall distribution of this signal across the whole cell population will be missed. This result points to the power of the technique to distinguish cell populations, determine their differences at the molecular level, and further, if desired, be used in multivariate classification.

To increase the sensitivity of the analysis, we utilized the solariX instrument's CASI capabilities, allowing for the accumulation of ion signal to increase sensitivity and dynamic range. Using the CASI technique, the number of ions measured and matched with LMSD and METLIN database increase to 771 and 400, respectively, leading to ~ 20 and 15% increase as compared to the results without using the CASI technique, suggesting that MALDI-CASI-FTICR-IMS provides a potential means to increase the sensitivity and thus the number of putative IDs from database searching in future studies. Details of the CASI experiment can be found in Supplementary Material.

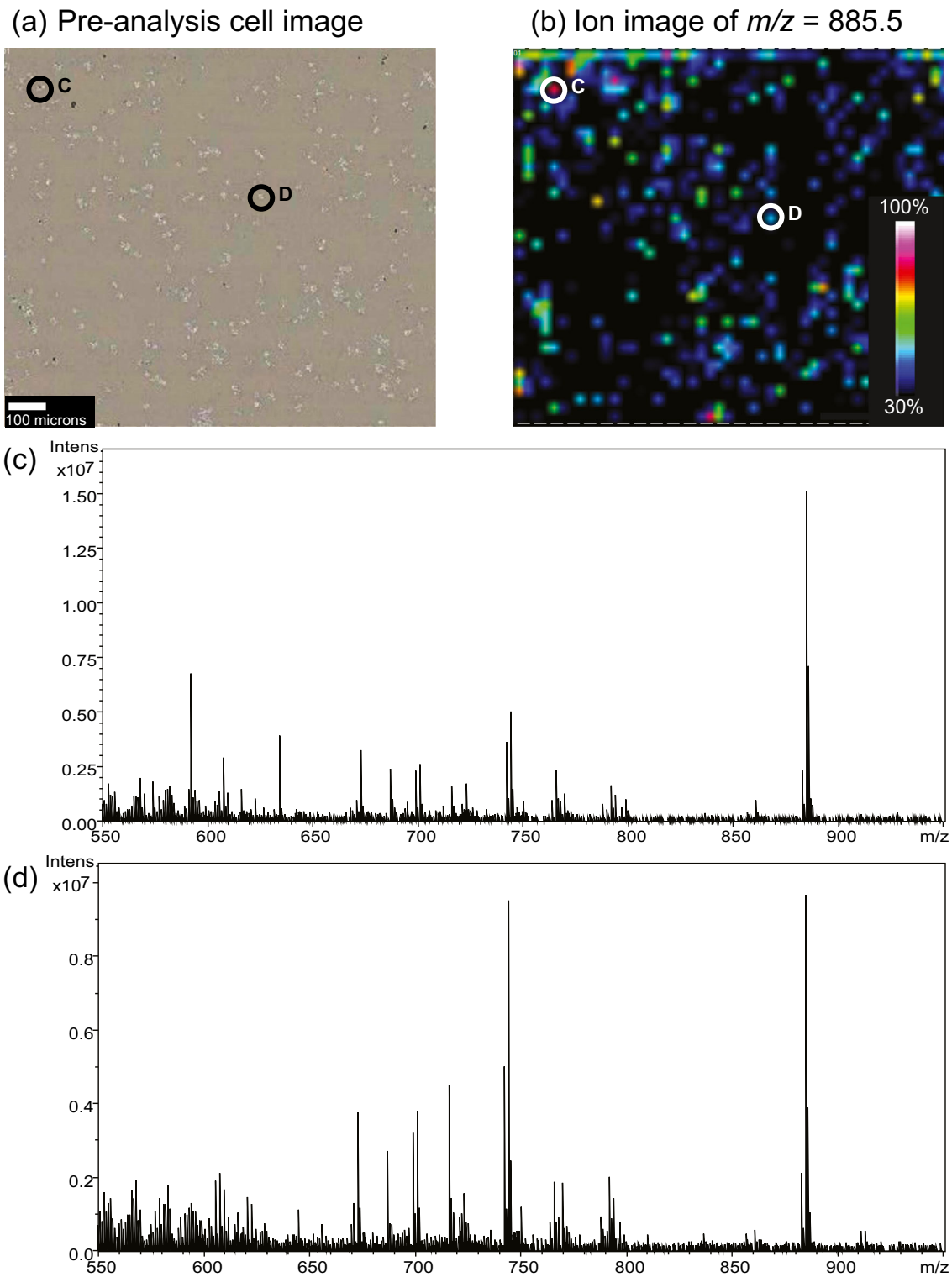

Figure 3. MALDI-IMS of normal RAW 264.7 cells. (a) High-resolution pre-analysis cell image. (b) Ion image corresponding to *m/z* = 885.55 of the sample area as in (a). (c), (d) Representative single-cell spectra extracted from two individual single cells highlighted in red and green circles in (a), respectively. (b)–(d) Heterogeneous molecular expression of each molecular species

Conclusion

The advanced mass spectrometry instrumentation and data processing tools described in this study provide a powerful opportunity to probe single cells and to characterize their complex role in the context of living systems. By applying this technology to normal and LPS-stimulated RAW 264.7 macrophage cells, we have

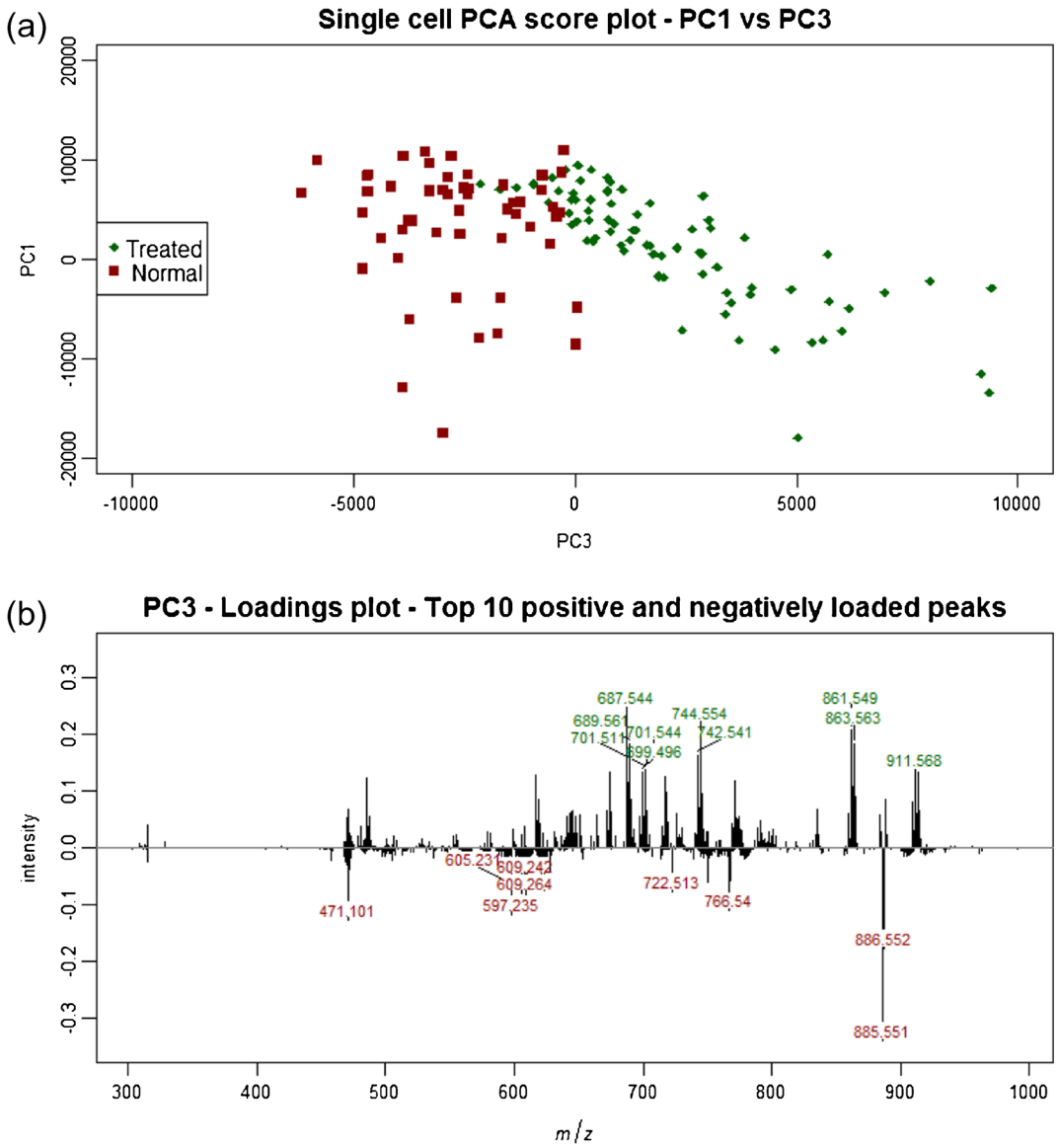

Figure 4. PCA score plot between the two cell conditions in the third principal component (PC3) (top). PC3 loadings plot of the top 10 most negative and positively loaded peaks (bottom)

observed up- or downregulation of lipids with a low or high degree of unsaturation, consistent with the trend observed in normal and diseased state tissues of breast, lung, colorectal, esophageal, gastric, and thyroid cancer as well as in glaucomatous aqueous humor [32, 33]. More importantly, we have measured variations (narrowed or

Table 1. Top Positive and Negatively Loaded Lipid Peaks of the Third Principle Component Determined by MALDI-FTICR-MS

Observed *m/z*	Species	Formula	Theoretical mass	Δppm
911.568	*[PI(40:5)-H]*$^-$	C49H85O13P	911.566	2.74
885.551	*[PI(38:4)-H]*$^-$	C47H83O13P	885.550	1.24
863.563	[PI(36:1)-H]$^-$	C45H85O13P	863.566	2.90
861.549	[PI(36:2)-H]$^-$	C45H83O13P	861.549	1.04
766.540	*[PE(38:4)-H]*$^-$	C43H78NO8P	766.539	1.21
744.554	[PE(36:1)-H]$^-$	C41H80NO8P	744.555	0.40
742.541	[PE(36:2)-H]$^-$	C41H78NO8P	742.539	2.42
722.513	*[PE(36:4)-H]*$^-$	C41H74NO7P	722.513	0.00
699.496	[PA(36:2)-H]$^-$	C39H73O8P	699.497	1.43
689.561	[SM(d18:0/15:0)-H]$^-$	C38H79N2O6P	689.560	1.02

Species with positive loading scores are shown in standard font, whereas those with negative loading scores are shown in italics

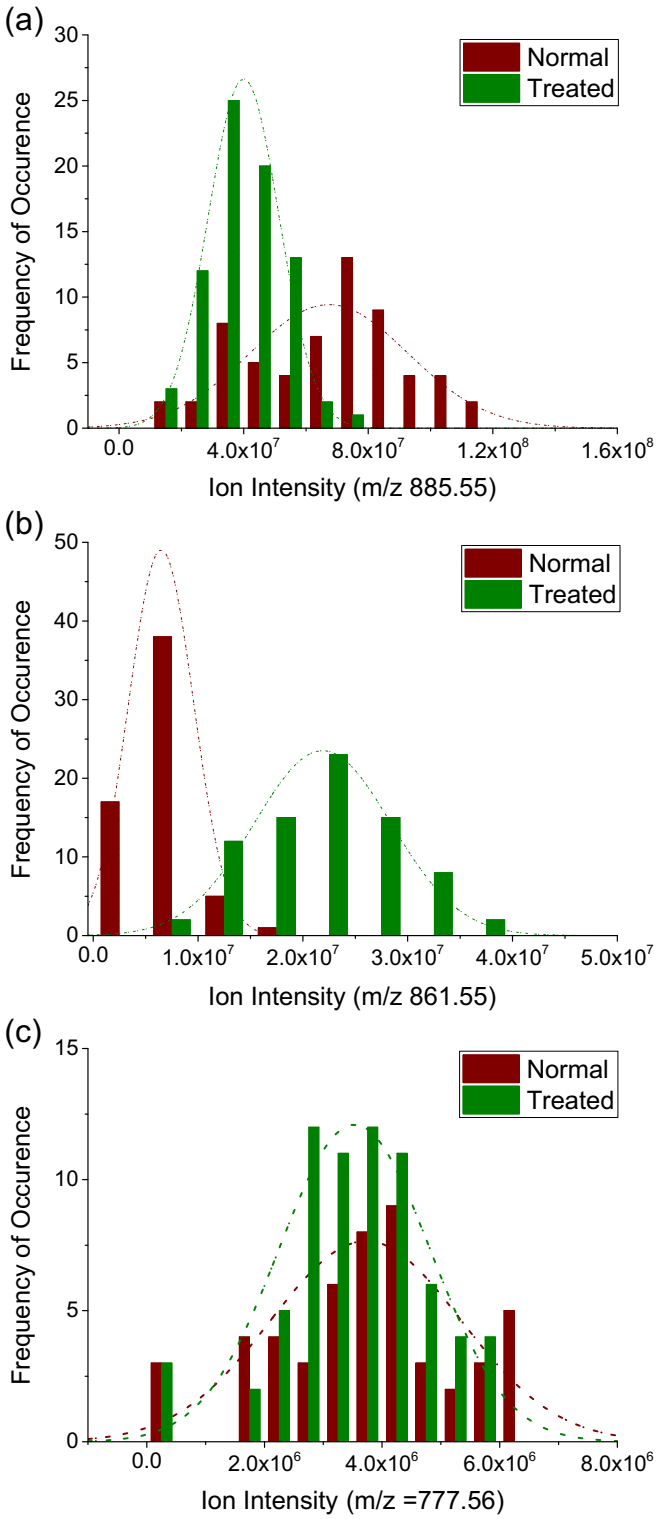

Figure 5. Histograms of ion abundances of *m/z* = 885.55 and 861.55, and 777.56 from normal ($n = 60$) and LPS-stimulated ($n = 70$) RAW 264.7 cells. These results show that LPS stimulation selectively influences the expression of selected molecular species at (a) *m/z* 885.55 and (b) *m/z* 861.55, shifting both the position of the mean and altering the shape of the distribution of ion abundance. The ion at (c) *m/z* 777.56 shows no evidence of altered expression upon LPS stimulation

widened) in the heterogeneity of these lipid expressions upon chemical stimulation of the cells, which will be missed using a population-level technique. In conclusion, the MALDI-FTICR-MS methodology described herein was demonstrated to advance sensitivity, specificity, spatial resolution, and throughput of single-cell lipidomics.

Acknowledgments

This work is supported by NIH grants R33DK105149 and P41GM103391. The authors acknowledge Nichole A. Lobdell from Eric P. Skaar Lab for cell culture. The authors also thank Eric C. Spivey for his careful reading of our manuscript and many insightful comments and suggestions.

References

1. Cai, L., Friedman, N., Xie, X.S.: Stochastic protein expression in individual cells at the single molecule level. Nature. **440**, 5 (2006)
2. Zenobi, R.: Single-cell metabolomics: analytical and biological perspectives. Science. **342**, 1243259 (2013)
3. Elowitz, M.B., Levine, A.J., Siggia, E.D., Swain, P.S.: Stochastic gene expression in a single cell. Science. **297**, 4 (2002)
4. Jansson, E.T., Comi, T.J., Rubakhin, S.S., Sweedler, J.V.: Single cell peptide heterogeneity of rat islets of Langerhans, *ACS Chem*. Biol. **11**, 8 (2016)
5. Lidstrom, M.E., Konopka, M.C.: The role of physiological heterogeneity in microbial population behavior. Nat. Chem. Biol. **6**, 8 (2010)
6. van Baarsen, L.G., Wijbrandts, C.A., Timmer, T.C., van der Pouw Kraan, T.C., Tak, P.P., Verweij, C.L.: Synovial tissue heterogeneity in rheumatoid arthritis in relation to disease activity and biomarkers in peripheral blood. Arthritis Rheum. **62**, 1602–1607 (2010)
7. Pelfrey, C.M., Rudick, R.A., Cotleur, A.C., Lee, J.C., Tary-Lehmann, M., Lehmann, P.V.: Quantification of self-recognition in multiple sclerosis by single-cell analysis of cytokine production. J. Immunol. **165**, 11 (2000)
8. Mannello, F., Ligi, D.: Resolving the cell heterogeneity of tumours and searching reliable protein cancer biomarkers in breast microenvironment. BMC Cancer. **13**, 8 (2013)
9. Gilbertson, R.J., Graham, T.A.: Cancer: resolving the stem-cell debate. Nature. **488**, 2 (2012)
10. Eberwine, J., Sul, J.-Y., Bartfai, T., Kim, J.: The promise of single-cell sequencing. Nat. Methods. **11**, 3 (2014)
11. Chandra, S.: Quantitative imaging of chemical composition in single cells by secondary ion mass spectrometry: cisplatin affects calcium stores in renal epithelial cells. Methods Mol. Biol. **656**, 28 (2010)
12. Waki, M., Ide, Y., Ishizaki, I., Nagata, Y., Masaki, N., Sugiyama, E., Kurabe, N., Nicolaescu, D., Yamazaki, F., Hayasaka, T., Ikegami, K., Kondo, T., Shibata, K., Hiraide, T., Taki, Y., Ogura, H., Shiiya, N., Sanada, N., Setou, M.: Single-cell time-of-flight secondary ion mass spectrometry reveals that human breast cancer stem cells have significantly lower content of palmitoleic acid compared to their counterpart non-stem cancer cells. Biochimie. **107**, 5 (2014)
13. Szakal, C., Narayan, K., Fu, J., Lefman, J., Subramaniam, S.: Compositional mapping of the surface and interior of mammalian cells at submicrometer resolution. Anal. Chem. **83**, 1207–1213 (2011)
14. Hua, X., Szymanski, C., Wang, Z., Zhou, Y., Ma, X., Yu, J., Evans, J., Orr, G., Liu, S., Zhu, Z., Yu, X.-Y.: Chemical imaging of molecular changes in a hydrated single cell by dynamic secondary ion mass spectrometry and super-resolution microscopy. Integr. Biol. **8**, 10 (2016)
15. Nemes, P., Vertes, A.: Laser ablation electrospray ionization for atmospheric pressure, in vivo, and imaging mass spectrometry. Anal. Chem. **79**, 9 (2007)
16. Onjiko, R.M., Moody, S.A., Nemes, P.: Single-cell mass spectrometry reveals small molecules that affect cell fates in the 16-cell embryo. Proc. Natl. Acad. Sci. U. S. A. **112**, 6 (2015)
17. Mellors, J.S., Jorabchi, K., Smith, L.M., Ramsey, J.M.: Integrated microfluidic device for automated single cell analysis using electrophoretic separation and electrospray ionization mass spectrometry. Anal. Chem. **82**, 7 (2010)
18. Liu, J.-X., Aerts, J.T., Rubakhin, S.S., Zhang, X.-X., Sweedler, J.V.: Analysis of endogenous nucleotides by single cell capillary electrophoresis-mass spectrometry. Analyst. **139**, 8 (2014)
19. Fukano, Y., Tsuyama, N., Mizuno, H., Date, S., Takano, M., Masujima, T.: Drug metabolite heterogeneity in cultured single cells profiled by picotrapping direct mass spectrometry. Nanomedicine (Lond). **7**, 10 (2012)
20. Masujima, T.: Live single-cell mass spectrometry. Anal. Sci. **25**, 8 (2009)
21. Pan, N., Rao, W., Kothapalli, N.R., Liu, R., Burgett, A.W.G., Yang, Z.: The single-probe: a miniaturized multifunctional device for single cell mass spectrometry analysis. Anal. Chem. **86**, 5 (2014)
22. Gong, X., Zhao, Y., Cai, S., Fu, S., Yang, C., Zhang, S., Zhang, X.: Single cell analysis with probe ESI-mass spectrometry: detection of metabolites at cellular and subcellular levels. Anal. Chem. **8**, 3809–3816 (2014)
23. Gholipour, Y., Erra-Balsells, R., Hiraoka, K., Nonami, H.: Living cell manipulation, manageable sampling, and shotgun picoliter electrospray mass spectrometry for profiling metabolites. Anal. Biochem. **433**, 9 (2012)
24. Amantonico, A., Oh, J.Y., Sobek, J., Heinemann, M., Zenobi, R.: Mass spectrometric method for analyzing metabolites in yeast with single cell sensitivity. Angew. Chem., Int. Ed. Engl. **47**, 4 (2008)
25. Li, L., Garder, R.W., Sweedler, J.V.: Single-cell MALDI: a new tool for direct peptide profiling. Trends Biotechnol. **18**, 151–160 (2000)
26. Lindström, S., Andersson-Svahn, H.: Overview of single-cell analyses: microdevices and applications. Lab Chip. **10**, 3363–3372 (2010)
27. Adams, D.O., Hamilton, T.A.: The cell biology of macrophage activation. Annu. Rev. Immunol. **2**, 283–318 (1984)
28. Morrison, D.C., Ryan, J.L.: Endotoxins and disease mechanisms. Annu. Rev. Med. **38**, 417–432 (1987)
29. Hankin, J.A., Barkley, R.M., Murphy, R.C.: Sublimation as a method of matrix application for mass spectrometric imaging. J. Am. Soc. Mass Spectrom. **18**, 1646–1652 (2007)
30. Yang, J., Caprioli, R.M.: Matrix sublimation/recrystallization for imaging proteins by mass spectrometry at high spatial resolution. Anal. Chem. **83**, 7 (2011)
31. Bemis, K.D., Harry A., Eberlin, L. S., Ferreira, C., van de Ven, S. M., Mallick, P., Stolowitz, M., Vitek O.: Cardinal: an R package for statistical analysis of mass spectrometry-based imaging experiments. Bioinformatics **31**, 2418–2420 (2015)
32. Guo, S., Wang, Y., Zhou, D., Li, Z.: Significantly increased monounsaturated lipids relative to polyunsaturated lipids in six types of cancer microenvironment are observed by mass spectrometry imaging. Sci. Rep. **4**, 5959 (2014)
33. Aljohani, A.J., Munguba, G.C., Guerra, Y., Lee, R.K., Bhattacharya, S.K.: Sphingolipids and ceramides in human aqueous humor. Mol. Vis. **19**, 1966–1984 (2013)